Characteristics of p-n Junction Detectors Based on Thermally-Grown Tellurium-Doped Silicon

Naseer K. Lazim

Department of Physics, College of Education, University of Kufah, Najaf, IRAQ

Abstract
In this work, the photoelectric properties of tellurium-doped silicon p-n junction were studied. Illumination of impurity absorption range influence on current-voltage and spectral characteristics of the fabricated device were considered. The photoresponse dependencies on electric intensity, current and radiation power at the sample were observed. Results obtained in this work showed that the current-sensitivity of the fabricated structures at forward bias is rather higher than that of photoresistors. The threshold photosensitivity and the detectivity were up to 2.85×10^{-16} W.Hz$^{-1/2}$ and 2.1×10^{11} cm.Hz$^{1/2}$W^{-1}, respectively.

Keywords: Silicon devices, Tellurium dopant, Heterojunction, Photoelectric properties
Received: 26 January 2024; **Revised:** 22 March 2024r; **Accepted:** 29 March 2024; **Published:** 1 April 2024

1. Introduction

The interest in the development of extrinsic photodetectors has been increased by the possibility of fabricating monolithic thermal imaging systems, photodetector arrays, charge-coupled devices, etc., based on extrinsic silicon. The fact that silicon integrated-circuit technology is highly developed facilitated the development of these devices [1-4].

The photoconducting properties of Te-doped silicon were first investigated in 1970's. The early work was characterized by low Te concentrations [5] and high compensation ratios [6] which lead to inferior detector performance. Tellurium is an n-type impurity, has low boiling point temperature and diffuses in silicon fast. These factors complicate the doping of silicon during silicon crystal growth, which occurs at ~1410°C but permit doping after crystal growth by closed quartz tube. The variables in a closed tube diffusion are the diffusion temperature, the quench procedure, the diffusion times and the diffusion vapor pressure [7].

In the present paper, the results of 3-5μm illumination of tellurium-doped silicon p-n structure were presented. It is shown that an effective injection amplification might be realized in the case of illumination from impurity range. The photodiode properties have been compared with silicon-tellurium (Si/Se) photoresistors those have the same geometrical sizes.

2. Experimental Part

Samples of (111) p-type boron-doped silicon were doped by tellurium at temperature of 1100°C in an evacuated quartz-tube. The concentration of residual atoms in initial silicon was determined to be about 10^{11}-10^{12} cm^{-2}. The samples were then etched for one minute in a HNO_3:HF:H_2O solution of 20:5:6 ratios. The concentration of electro-active tellurium atoms in silicon after doping process was about 6×10^{16} cm^{-3}. The maximum photoresponse at temperature of 263K was observed at wavelength (λ_p) of about 3.8 μm and the long-wave boundary level corresponding to 50% relative spectral characteristics ($\lambda_{1/2}$) was about 4.2 μm. The optical-ionization energy (ΔE_{op}) level of tellurium was about 0.301 eV.

3. Results and Discussion

The I-V characteristics of samples at T=300K had the usual low power rectifier

form. At T=263K a negative resistance region on I-V characteristics was formed in the forward direction as shown in Fig. (1). An Ohmic region was observed when illumination was absent and injection was low. By increasing the voltage, the region changes into a $J \approx V^{3/2}$ region. The dependence $J \approx V^{3/2}$ changed into a linear one at large injection levels after which impact ionization began.

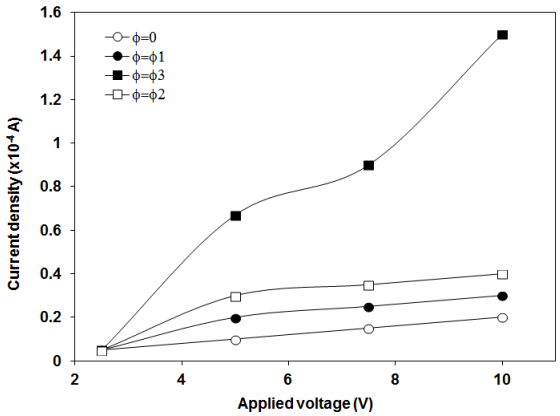

Fig. (1) Illumination-dependent current-voltage (I-V) characteristics of tellurium-doped silicon photodiode structure at different injection levels (φ), where $\varphi_1<\varphi_2<\varphi_3$

Figure (2) indicates the behavior of sensitivity (R) as the wavelength incident on the photodiode (or photoresistive) increases. It is clear that the sensitivity has a maximum at a certain wavelength, which could be considered the operative wavelength of such photodiode.

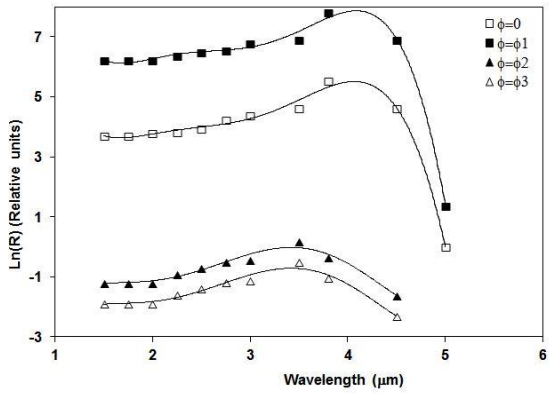

Fig. (2) Spectral characteristics *vs.* incident wavelength on the fabricated photodiodes and equivalent photoresistors

The behaviors of curves in figures (3) and (4) correspond to each other, which makes an evidence of the amplification mechanisms. A sharp sensitivity growth of particular samples was observed at distribution point and sensitivity increased for several times in this region, as shown in Fig. (5).

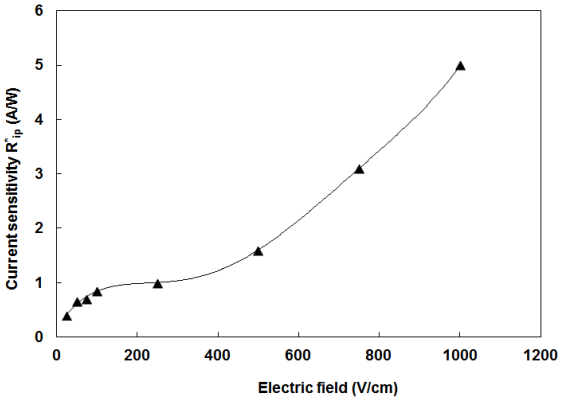

Fig. (3) Variation of current sensitivity with the applied electric field for the fabricated photodiodes

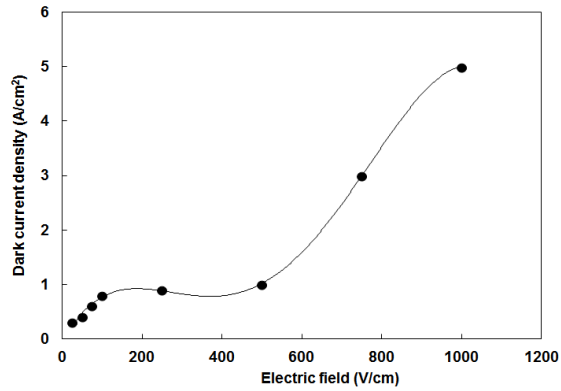

Fig. (4) Variation of the dark current density with the applied electric field for the fabricated photodiodes

Figure (5) shows the variation of current sensitivity with the applied electric field. Similarly, figure (6) shows the variation of dark current density with the applied electric field and the same behavior is observed below 200 V/cm and then the dark current density tends to be constant during the range 200-800 V/cm within 75-90 A/cm^2. Such behavior is preferred to recognize the characteristics of the fabricated photodiode in the same range of applied electric fields considered for optimum operation. Similarly, the dark current density begins to increase beyond applied electric field of 10^3 V/cm.

The voltage sensitivity was observed at about 2×10^9 V/W ($R=R_{PD}$) and then the detectivity of photodiode was measured too.

Radiation of thermal source (T=500K) at the receiver temperature of 263K and at the field-of-view (FOV) on the background 60° was also used. For the applied field of about 10 V/cm, the specific detectivity (D^*) was about $8x10^9$ cm.Hz$^{1/2}$/W. Practically, at electric fields of 5-6 $x10^2$ V/cm, the specific detectivity was not changed, although such a sensitivity increased abruptly, but in that case the noise-level increased as well.

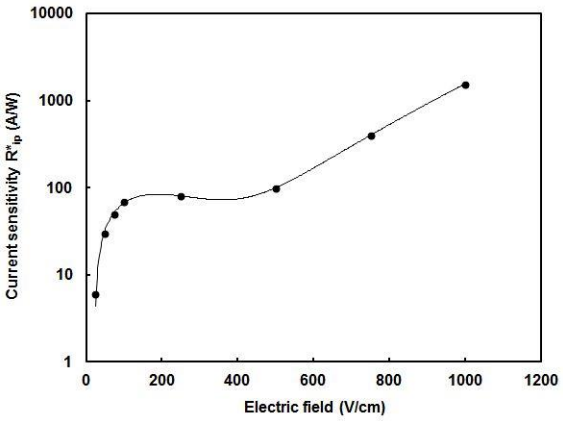

Fig. (5) variation of the current sensitivity with the applied electric field for the fabricated photoresistors

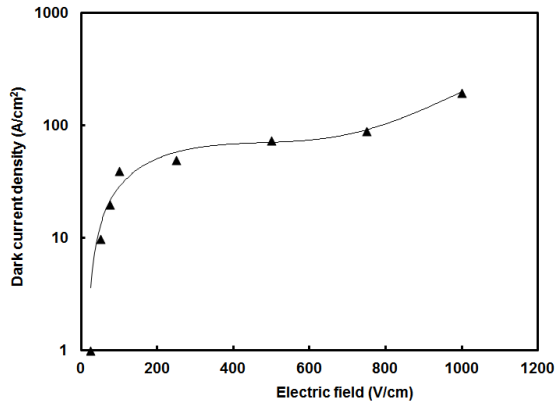

Fig. (6) Variation of the dark current density with the applied electric field for the fabricated photoresistors

An idealized curve of relative spectral sensitivity with a peak wavelength of 3.8 μm was used to define the absolute spectral detectivity and further D^*_{max}/D^*_{500} was calculated. In this case, the relation was equal to 12.5 and $D^*_{max} \approx 10^{11}$ cm.Hz$^{1/2}$/W at 60° field-of-view.

The magnitude of sensitivity and detectivity did not depend on frequency in the range around 200 kHz. Increasing detectivity with decreasing field-of-view on a background up to 30° was registered to be about $2.1x10^{11}$ cm.Hz$^{1/2}$/W.

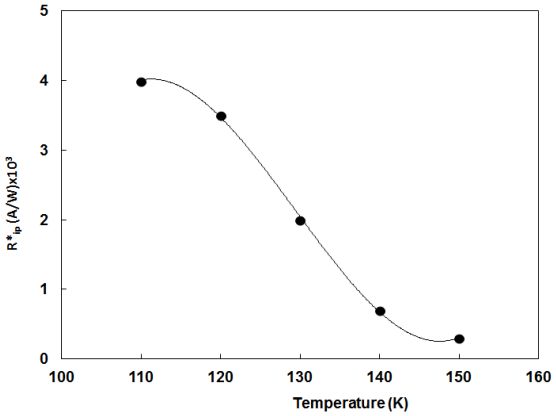

Fig. (10) Variation of the current sensitivity with temperature for fabricated tellurium-doped silicon photodiode

4. Conclusions

From the results presented in this work, we could conclude that a negative resistance region on the I-V characteristics and Ohmic region were observed in the forward bias at no-illumination and low-injection condition. After the beginning of an impact ionization, an I-V characteristics region was observed in which the voltage did not depend on current for most diodes. Most photodiodes had high photosensitivity near the breakdown point. Detectivity increased with the decreasing of the field-of-view. Tellurium-doped silicon diode structures can successfully be used as radiation photoreceivers in the atmospheric window 3-5 μm with a reasonable efficiencies.

References

[1] D. L. Mathine, **The integration of III-V optoelectronics with silicon circuitry,** *IEEE J. Selec. Top. Quantum Electron.*, 3, p. 952, (1997).

[2] F. P. Widdershoven, J. Haisma, J. Naus, Boron contamination and antimony segregation at the interface of directly bonded silicon wafers, *J. Appl. Phys.* 68, p. 6253, (1990).

[3] F.J. Al-Maliki, O.A. Hammadi and E.A. Al-Oubidy, "Optimization of Rutile/Anatase Ratio in Titanium Dioxide Nanostructures prepared by DC Magnetron Sputtering Technique", Iraqi J. Sci., 60 (2019) 91-98.

[4] J. Dresner and F.V. Shallcross, "Crystallinity and Electronic Properties of Evaporated CdS Films", J. Appl. Phys., 34(8) (1963) 2390.

[5] B. Levine, C. J. Pinzone, S. Hui, C. A. King, R. E. Leibenguth, D. R. Zolnowski, D. V. Lang, H. W. Krautter, M. Geva, Ultralow-dark-current wafer-bonded Si/InGaAs photodetectors, *Appl. Phys. Lett.* 75, p. 2141 (1999).

[6] Oday A. Hamadi, Khaled Z. Yahiya, "Optical and electrical properties of selenium-antimony heterojunction formed on silicon substrate", Sharjah Univ. J. Pure Appl. Sci. (UoS J PAS), 4(2), 2007, 1-11.

[7] A. Berthold, B. Jakoby, M. J. Vellekoop, Wafer-to-wafer fusion bonding of oxidized silicon to silicon at low temperatures, *Sensors & Actuators*, A68, p. 410, (1998).

[8] Oday A. Hamadi, Ban A.M. Bader, Afnan K. Yousif, "Electrical Characteristics of Silicon p-n Junction Solar Cells Produced by Plasma-Assisted Matrix Etching Technique", Eng. Technol. J., 28, 2008, 995-1001.

[9] P. Kopperschmidt, G. Kästner, D. Hesse, N. D. Zakharov and U. Gösele, High bond energy and thermomechanical stress in silicon on sapphire wafer bonding, *Appl. Phys. Lett.* 70 (22), pp. 2972-2974 (1997).

[10] O.A. Hammadi, F.J. Al-Maliki and E.A. Al-Oubidy, "Photocatalytic Activity of Nitrogen-Doped Titanium Dioxide Nanostructures Synthesized by DC Reactive Magnetron Sputtering Technique", Nonlinear Opt. Quantum Opt., 51 (1-2) (2019) 67-78.

[11] Afnan K. Yousif, Oday A. Hamadi, "Plasma-Induced Etching of Silicon Surfaces", Bulg. J. Phys., 35(3), 2008, 191-197.

[12] A. Hawkins, W. Wu, P. Abraham, K. Streubel, J. E. Bowers, High Gain-Bandwidth-Product Silicon Heterointerface Photodetector, *Appl. Phys. Lett.*, 70, p. 303, (1996).

[13] Oday A. Hamadi, "Characteristics of CdO-Si Heterostructure Produced by Plasma-Induced Bonding Technique", Proc. IMechE, Part L, J. Mater.: Design and Applications, 222, 2008, 65-71, DOI: 10.1243/14644207JMDA56.

[14] A. Fontcuberta i Morral, J.M. Zahler and H.A. Atwater, InGaAs/InP double heterostructures on InP/Si templates fabricated by wafer bonding and hydrogen-induced exfoliation, *Appl. Phys. Lett.* 83 (26), pp. 5413-5415 (2003).

[15] M. Sugo, Y. Takanashi, M. M. Al-Jassim, M. Yamaguchi, Heteroepitaxial growth and characterization of InP on Si substrates, *J. Appl. Phys.* 68, 2, p. 540-547, (1990).

[16] Oday A. Hamadi, "Effect of Annealing on the Electrical Characteristics of CdO-Si Heterostructure Produced by Plasma-Induced Bonding Technique", Iraqi J. Appl. Phys. (IJAP), 4(3), 2008, 34-37.

[17] D. S. Wuu, R. H. Horng, M. K. Lee, Indium phosphide on silicon heteroepitaxy: Lattice deformation and strain relaxation, *J. Appl. Phys.* 68, 7, pp. 3338, (1990).

[18] Aseel A.K. Hadi, Oday A. Hamadi, "Optoelectronic Characteristics of As-doped Silicon Photodetectors Produced by LID Technique", Iraqi J. Appl. Phys. Lett. (IJAPLett), 1(2), 2008, 23-26.

[19] Oday A. Hammadi, "Photovoltaic Properties of Thermally-Grown Selenium-Doped Silicon Photodiodes for Infrared Detection Applications", Photonic Sensors, 5(2), 2015, 152-158, DOI: 10.1007/s13320-015-0241-4

[20] Oday A. Hammadi, Mohammed K. Khalaf, Firas J. Kadhim, "Silicon Nitride Nanostructures Prepared by Reactive Sputtering Using Closed-Field Unbalanced Dual Magnetrons", Proc. IMechE, Part L, J. Mater.: Design and Applications, Accepted for publication: July 2015, DOI: 10.1177/1464420715601151.

[21] Oday A. Hammadi, Mohammed K. Khalaf, Firas J. Kadhim, "Fabrication of UV Photodetector from Nickel Oxide Nanoparticles Deposited on Silicon Substrate by Closed-Field Unbalanced Dual Magnetron Sputtering Techniques", Opt. Quantum Electron., 47(12), 2015, 3805-3813. DOI: 10.1007/s11082-015-0247-6

[22] Oday A. Hammadi, Mohammed K. Khalaf, Firas J. Kadhim, "Fabrication and Characterization of UV Photodetectors Based on Silicon Nitride Nanostructures Prepared by Magnetron Sputtering", Proc. IMechE, Part N, J. Nanoeng. Nanosys., accepted for publication: September 3rd 2015.

[23] O.A. Hammadi, M.K. Khalaf, F.J. Kadhim, B.T. Chiad, "Operation Characteristics of a Closed-Field Unbalanced Dual-Magnetrons Plasma Sputtering System", Bulg. J. Phys., 41(1) (2014) 24-33.

[24] O.A. Hammadi, "Production of Nanopowders from Physical Vapor Deposited Films on Nonmetallic Substrates by Conjunctional Freezing-Assisted Ultrasonic Extraction Method", Proc. IMechE, Part N, J. Nanomater. Nanoeng. Nanosys., 232(4) (2018) 135-140.

[25] H. Itakura, T. Suzuki, Z.K. Jiang, T. Soga, T. Jimbo and M. Umeno, Effect of InGaAs/InP strained layer superlattice in InP-on-Si, *J. Cryst. Growth*, 115, p.154-157, (1991).

